

# Dynamics of connective-tissue localization during chronic *Borrelia burgdorferi* infection

Denise M Imai, Sunlian Feng, Emir Hodzic and Stephen W Barthold

The etiologic agent of Lyme disease, *Borrelia burgdorferi*, localizes preferentially in the extracellular matrix during persistence. In chronically infected laboratory mice, there is a direct association between *B. burgdorferi* and the proteoglycan decorin, which suggests that decorin has a role in defining protective niches for persistent spirochetes. In this study, the tissue colocalization of *B. burgdorferi* with decorin and the dynamics of borrelial decorin tropism were evaluated during chronic infection. Spirochetes were found to colocalize absolutely with decorin, but not collagen I in chronically infected immunocompetent C3H mice. Passive immunization of infected C3H-*scid* mice with *B. burgdorferi*-specific immune serum resulted in the localization of spirochetes in decorin-rich microenvironments, with clearance of spirochetes from decorin-poor microenvironments. In passively immunized C3H-*scid* mice, tissue spirochete burdens were initially reduced, but increased over time as the *B. burgdorferi*-specific antibody levels waned. Concurrent repopulation of the previously cleared decorin-poor microenvironments was observed with the rising tissue spirochete burden and declining antibody titer. These findings indicate that the specificity of *B. burgdorferi* tissue localization during chronic infection is determined by decorin, driven by the borrelia-specific antibody response, and fluctuates with the antibody response.

*Laboratory Investigation* (2013) 93, 900–910; doi:10.1038/labinvest.2013.81; published online 24 June 2013

**KEYWORDS:** *Borrelia burgdorferi*; decorin; decorin-binding proteins; Lyme disease; mouse model

*Borrelia burgdorferi*, the causative agent of Lyme borreliosis, is a tick-transmitted spirochete that establishes chronic extracellular infection in mammalian hosts.<sup>1,2</sup> Lyme borreliosis progresses through multiple loosely defined stages, including local infection, dissemination, and persistence.<sup>1</sup> During initial tick-borne infection, spirochetes are deposited within the dermis, locally proliferate, and then disseminate to distant tissues.<sup>3–5</sup> Distant dissemination is followed by or occurs simultaneously with the onset of acquired immunity, which resolves disease (ie, arthritis and carditis) and reduces the number of spirochetes in tissue.<sup>6</sup> Remaining spirochetes that have evaded the acquired immune response persist for months to years.<sup>7–10</sup> At each of these stages, morphologically intact spirochetes are identifiable in the extracellular matrix (ECM). During early infection, disseminating spirochetes colonize a broad range of tissues.<sup>1,3,6</sup> During chronic infection, persisting spirochetes are restricted to the ECM of the dermis, periarticular connective tissue, tendons, ligaments, perineurium, periaortic connective tissue at the base of the heart, and other collagen-rich sites.<sup>3,4,6,7,11–13</sup>

Since the initial disease description, spirochetes have been described as aligning with or intercalated between collagen fibers in the ECM of connective tissue.<sup>3,6,7,14</sup> Collagen is but one component of the molecularly diverse ECM. The ECM is composed of a network of fibrillar proteins embedded within a hydrated ground substance composed of proteoglycans and glycosaminoglycans.<sup>15</sup> In order to colonize these connective tissue-rich predilection sites, any bacterium, including a spirochete, must interact with these various ECM components through bacterial cell surface adhesins.<sup>16</sup> *B. burgdorferi* encodes a surprisingly large number of ECM adhesins for its relatively small genome (reviewed by Antonara *et al*<sup>17</sup>). The known borrelial ECM adhesins include decorin-binding protein (Dbp)A and B, *Borrelia* glycosaminoglycan-binding protein (Bgp), fibronectin-binding protein (BBK32), RevA, RevB, members of the *Borrelia* membrane protein family (BmpA–D), OspEF-related proteins (Erps), P66, and a yet to be identified adhesin that binds directly to type I collagen. These adhesins bind respectively to decorin, various glycosaminoglycans,

Center for Comparative Medicine, School of Veterinary Medicine, University of California, Davis, CA, USA

Correspondence: Dr SW Barthold, DVM, PhD, Center for Comparative Medicine, School of Veterinary Medicine, University of California, One Shields Avenue, Davis, CA 95616, USA.

E-mail: swbarthold@ucdavis.edu

Received 12 April 2013; revised 28 May 2013; accepted 29 May 2013

fibronectin, laminin, and  $\alpha_{11b}\beta_3$  and  $\alpha_v\beta_3$  integrins.<sup>17–25</sup> Based on the number of putative borrelial adhesins, many more borrelial adhesin–ECM ligand interactions are likely to be revealed in future.<sup>17,26</sup>

Given the wealth of adhesins elaborated by *B. burgdorferi*, it is not surprising that no single adhesin is absolutely essential to infection and persistence.<sup>2,17</sup> Lack of a single adhesin can alter pathogenicity by influencing specific stages of disease. For example, DbpA/B and decorin is one adhesin–ligand interaction that has been scrutinized in relation to chronic infection. Liang *et al*<sup>27</sup> observed a direct relationship between the numbers of persisting spirochetes and decorin expression level in collagen-rich tissues (eg, skin, joint, and heart). The observed protective capacity of these tissues was specific to decorin, evident only in the face of an acquired immune response, and associated with an increased expression of *dbpA*.<sup>27</sup> In chronic (post-disease resolution) infection, Barthold *et al*<sup>6</sup> demonstrated that the antibody-mediated immune response resulted in a change in the microenvironmental localization of persisting spirochetes into collagen-rich connective tissues. Together, these observations support the existence of preferential connective-tissue localization during chronic Lyme borreliosis. They further suggest that preferential connective-tissue localization may be driven by the humoral immune response and that decorin may be a major determining ECM component.

The purpose of this study was to evaluate the micro-environmental dynamics of connective-tissue localization in chronic stages of Lyme borreliosis in the mouse model, evaluate the influence of the *B. burgdorferi*-specific antibody response on the specificity of tissue localization, and evaluate the extent to which decorin determines connective-tissue localization. We focused on the heart and, in particular, the connective tissue of the heart base, as a model tissue for study, as it is a consistent site into which disseminating spirochetes colonize and a site in which inflammation (carditis) develops during the early phase of infection.<sup>3,4,11</sup> After induction of the immune response, the heart base is also a site in which disease resolves, but spirochetes persist within connective tissue.<sup>6,7</sup> Additionally, the heart base contains closely apposed decorin-rich (vascular adventitia) and decorin-poor (vascular media) microenvironments that other tissues, such as joints, lack. An added advantage of focusing on the heart base is that decalcification, which can result in inadequate antigen preservation, is not necessary. Using the heart in a well-characterized C3H<sup>7</sup> and passively immunized C3H-*scid*<sup>6,27–29</sup> mouse model of chronic Lyme borreliosis, the present study confirmed the preferential connective-tissue localization of *B. burgdorferi* and demonstrated that preferential connective-tissue localization is specific to decorin-rich microenvironments, is driven by a *B. burgdorferi*-specific antibody response, and that recrudescence results in loss of decorin-specific connective-tissue localization.

## MATERIALS AND METHODS

### Borrelial Strains

The low passage *B. burgdorferi* ‘*sensu stricto*’ strains cN40 and B31 were utilized to establish infections.<sup>7,30,31</sup> *B. burgdorferi* cultures were grown in liquid modified Barbour–Stoenner–Kelly (BSKII) medium supplemented with 6% normal rabbit serum.<sup>32</sup>

### Mice

Specific-pathogen-free, 3–5-week-old, female C3H/HeN (C3H) mice were acquired from Frederick Cancer Research Center (Frederick, MD, USA) and severe combined immunodeficient C3H/Smn.C1crHsd-*Prkdc*<sup>*scid*</sup> (C3H-*scid*) mice were obtained from Harlan Sprague Dawley (Indianapolis, IN, USA). Mice were killed by carbon dioxide narcosis and cardiac exsanguination.

### Experimental Infections

Mice were infected by subdermal inoculation of 10<sup>4</sup>–10<sup>5</sup> mid-log phase *B. burgdorferi* in 0.1 ml BSKII medium on the dorsal thoracic midline. To represent naive mice, uninfected mice were necropsied without borrelial inoculation. To represent chronic infection, C3H mice were necropsied at day 60 post inoculation. For passive immunization studies to manipulate humoral immunity, immune serum from C3H mice infected with either *B. burgdorferi* cN40 or B31 was collected at 60 days of infection, as previously described.<sup>29</sup> Infected C3H-*scid* mice were passively immunized with 0.3 ml immune serum subcutaneously on days 12, 18 and 24 post inoculation. Immune serum administered was homologous to the specific *B. burgdorferi* strain (cN40 or B31) used to establish infection. Negative controls were administered normal mouse serum (NMS) from uninfected naive mice. Subsets of passively immunized C3H-*scid* mice were necropsied on days 28, 56 and 72 post inoculation. Sub-inoculation site and urinary bladder tissues were aseptically collected for culture to confirm infection, as previously described.<sup>7</sup> Tissues collected for DNA extraction included skin, heart base, ventricular muscle, quadriceps muscle, and left tibiotarsus. Tissues collected for immunohistochemistry (IHC) and immunofluorescence (IF) included heart base and myocardium. Hearts were bisected along the longitudinal axis to provide samples for both DNA extraction, IHC and IF. Mice used in infectivity experiments that were neither culture- nor quantitative PCR (qPCR)-positive were discarded from the data set.

### Quantitative PCR

DNA was extracted from tissues using DNeasy tissue kits, according to the manufacturer’s instructions (QIAGEN, Valencia, CA, USA). Samples were analyzed by qPCR for *B. burgdorferi* flagellin (*flaB*) DNA, using a previously optimized primer set and internal hydrolysis probe assay<sup>33</sup> to confirm infection and quantify tissue spirochete burdens. Quantification of gene copies was based on absolute standard

curves prepared using plasmid standards.<sup>33</sup> Target-gene copy numbers were expressed as copy number of *flaB* per mg of tissue weight.

### Enzyme-Linked Immunosorbent Assay

Ninety-six-well plates were coated with 1  $\mu\text{g/ml}$  *B. burgdorferi* cN40 whole-cell lysate or 0.5  $\mu\text{g/ml}$  rabbit anti-mouse IgG antibody (Southern Biotech, Birmingham, AL, USA) in carbonate coating buffer (pH 9.6), as described previously.<sup>34</sup> The secondary antibody used was alkaline phosphatase-conjugated goat anti-mouse IgG, diluted at 1:5000 (Jackson ImmunoResearch Laboratories Inc., West Grove, PA, USA). Antibody-binding was revealed using 1 mg/ml phosphate substrate (Sigma-Aldrich, St Louis, MO, USA) in diethanolamine buffer. Optical density values (405 nm) were measured on a kinetic microplate reader (Molecular devices, Sunnyvale, CA, USA), as described previously.<sup>6</sup> Immune sera and individual mouse serum samples from passively immunized C3H-*scid* mice were titrated in three-fold dilutions (starting at 1:300) for immunoreactivity to either *B. burgdorferi* cN40 or for total serum IgG levels. All serum samples were tested in duplicate, and each assay included uninfected mouse serum (NMS from C3H and/or C3H-*scid* mice, as needed) as a negative control and day 60-post inoculation *B. burgdorferi* cN40-infected mouse immune serum as a positive control.

### Immunofluorescence

Tissues were embedded in Tissue-Tek OCT compound (Sakura, Torrance, CA, USA), flash-frozen in liquid nitrogen and stored at  $-80^{\circ}\text{C}$ . Tissues were sectioned 5- $\mu\text{m}$  thick on Superfrost/Plus slides (Thermo Fisher Scientific, Waltham, MA, USA), fixed for 5 min in cold acetone, air-dried for 30 min and rehydrated in PBS for 10 min. Non-specific reactivity was blocked by incubation with 10% horse serum in PBS for 30 min. Tissue sections were incubated with primary goat anti-decorin antibody (R&D systems, Minneapolis, MN, USA) for 12 h at  $4^{\circ}\text{C}$ . Primary antibody reactivity was assessed by incubation with the appropriate NorthernLights 493 fluorochrome-labeled secondary donkey anti-goat antibody (R&D systems) for 1 h at room temperature. Rinses were performed in PBS with 0.05% Tween 20 (Sigma-Aldrich) to reduce surface tension. Tissues were counterstained with DAPI for 10 min, mounted in Fluoromount-G (Southern Biotech, Birmingham, AL, USA) and cover-slipped.

### Histochemistry and IHC

Tissues were immersion-fixed in 10% neutral-buffered formalin, processed, paraffin-embedded, and sectioned 5- $\mu\text{m}$  thick onto Superfrost/Plus slides. Prior to processing, the heart base aorta was appropriately oriented in HistoGel (Thermo Scientific Richard-Allan Scientific, Kalamazoo, MO, USA). Sections of heart base (including aorta) were stained for connective tissue with Masson's trichrome. Sections of heart base (including aorta) were evaluated for the presence

of *B. burgdorferi*, as described previously<sup>29</sup> with the following modifications. Sections were incubated with the following primary antibodies, polyclonal immune serum from *B. burgdorferi*-infected rabbits or polyclonal rabbit anti-collagen I antibody (Abcam, Cambridge, MA, USA) or goat anti-decorin antibody (R&D systems), for 12 h at  $4^{\circ}\text{C}$ . The secondary goat anti-rabbit EnVision+ system-HRP (DAKO, Carpinteria, CA, USA) antibody was pre-conjugated to a non-avidin/biotin horseradish peroxidase-labeled polymer. A secondary anti-goat streptavidin-biotin immunoenzymatic detection system (Goat Cell and Tissue Staining Kit, R&D systems) was utilized, per manufacturer's instructions. Rinses were performed in PBS with 0.05% Tween 20 to reduce surface tension. Each immunohistochemical run was performed with the inclusion of a negative (by omission of the primary antibody) and positive (tissues from infected C3H-*scid* mice in which spirochetes were previously identified by IHC) control.

Sagittal sections through the heart, including the aorta at the heart base, were examined for the presence of spirochetes in the heart base and ventricular myocardium in the following microenvironments: tunica adventitia (connective tissue surrounding arteries), tunica media (the smooth muscle wall of arteries), and myocardial connective tissue. The myocardial connective tissue microenvironment included the myocardial interstitium, epicardium and connective tissue at the heart base (not associated with the great vessels). The anatomic sites and microenvironments were defined based on previous observations of borrelial distribution in the cardiovascular system.<sup>4,11,29</sup> Numbers of spirochetes within anatomic locales were graded on a scale of 0 (no spirochetes), 0.5 (rare spirochetes), 1 (small numbers), 2 (moderate numbers), and 3 (large numbers). The mean score  $\pm$  standard error (s.e.m.) was calculated for each treatment group. Tissue sections were blindly examined, without knowledge of treatment group, by a single pathologist.

### Image Acquisition

Epifluorescent and brightfield images were acquired on a Zeiss Axioskop microscope with a Zeiss AttoArc HBO 100 W mercury lamp, Zeiss filter sets, Zeiss Axiocam camera and Zeiss Axiovision software. All image manipulations, including resizing, white-balance adjustment, brightness adjustment (equivalent across epifluorescent images), arrowheads and added text were performed in Adobe Photoshop CS4.

### Statistics

Analyses were performed using independent samples *t*-test or one-way analysis of variance, followed by *post hoc* pair-wise comparisons (Tukey's HSD test) (Prism v. 5, GraphPad software). Calculated *P*-values  $\leq 0.05$  were considered significant.

## RESULTS

### Localization of *B. burgdorferi* in the Tunica Adventitia and Myocardial Connective Tissue During Chronic Infection

To begin evaluation of spirochetal connective-tissue localization during chronic infection, the specific cardiovascular microenvironments in which *B. burgdorferi* persist were investigated. Borrelial infection was maintained in 10 immunocompetent C3H mice inoculated with *B. burgdorferi* strain cN40 for 60 days, a time point at which immune-mediated disease resolution and reduction of spirochete burdens in tissues has occurred.<sup>33</sup> Distribution of spirochetes within (i) anatomic sites (heart base *versus* ventricular myocardium) and (ii) microenvironments (tunica adventitia, tunica media, and myocardial connective tissue) was evaluated by IHC. A very small number of spirochetes were found (Figure 1) randomly distributed throughout the heart. Though no anatomic site specificity (heart base *versus* myocardium) was observed, microenvironmental specificity was apparent. The only microenvironments in which spirochetes were identified were in the tunica adventitia (Figure 1a) and myocardial connective tissue (Figure 1b). No spirochetes were identified within the tunica media.

### Spirochete Localization in the Tunica Adventitia and Myocardial Connective Tissue is Induced by the *B. burgdorferi*-Specific Antibody Response

The original descriptions of spirochete distribution after antibody-mediated disease resolution<sup>6,27,29,35</sup> were made using strain N40 or B31. However, the microscopic localization of morphologically intact spirochetes has only been reported with *B. burgdorferi* N40. DbpA-N40 and DbpA-B31 have only an 81% amino-acid sequence similarity,<sup>36</sup> with variable *in vitro* decorin-binding abilities.<sup>37,38</sup> Thus, the influence of the DbpA/B-decorin

interaction and connective-tissue localization could potentially be strain-specific. Therefore, evaluation of spirochete localization post disease resolution was performed using strain B31, to compare with the N40 archetype in order to account for possible strain-specific variation in microenvironmental localization.<sup>6</sup>

To evaluate the contribution of humoral immunity to the microenvironmental specificity (and potential preferential connective-tissue localization) of borrelial persistence, 10 immunodeficient C3H-*scid* mice were inoculated with *B. burgdorferi* strain B31. A subset of five mice was passively immunized with B31-specific immune serum and a subset of five mice was administered serum from uninfected mice (NMS). At necropsy on day 28 post inoculation, a very small number of spirochetes were identified within the tunica adventitia and myocardial connective tissue (Table 1) in the mice treated with B31-specific immune serum, in contrast to mice treated with NMS, in which spirochetes could be identified in all microenvironments. Relative spirochete burden scores in these microenvironments were statistically significantly lower in mice treated with immune serum (all *P*-values  $\leq 0.05$ ) than in the heavily colonized C3H-*scid* mice administered NMS (Table 1). The tunica media of C3H-*scid* mice treated with immune serum was cleared of spirochetes, while the tunica media of mice administered NMS was not. Thus, in passively immunized C3H-*scid* mice, the distribution of spirochetes on day 28 recapitulated the distribution of persistent spirochetes in immunocompetent mice, the distribution of persistent N40 spirochetes, and reaffirmed the accuracy with which passive immunization reproducibly induces antibody-mediated tissue spirochete reduction and microenvironmental location for persistence.<sup>27–29,35</sup> The data supported the hypothesis that microenvironment-specific localization of persistent spirochetes is associated with a *B. burgdorferi*-specific antibody response.

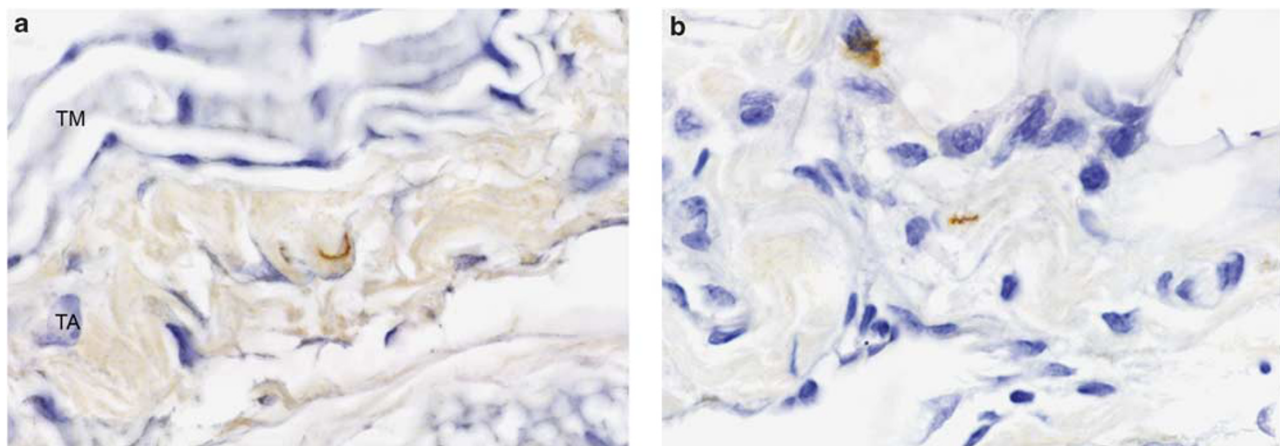


**Figure 1** In chronic infection, spirochetes localized to the tunica adventitia (TA) (a) and myocardial connective tissues (b) in the cardiovascular tissue of a C3H mouse, 60 days post inoculation with *B. burgdorferi*. The tunica media (TM) was devoid of spirochetes. Indirect IHC with rabbit anti-*B. burgdorferi* immune serum and immunoperoxidase reaction with 3, 3'-diaminobenzidine (DAB) substrate; hematoxylin counterstain;  $\times 40$ .

### Decorin and *B. Burgdorferi* Colocalize in the Tunica Adventitia and Myocardial Connective Tissue during Chronic Infection

The observed microenvironmental specificity of persistent spirochetes in response to *B. burgdorferi*-specific antibody suggested differences in the composition of the tunica adventitia and myocardial connective tissue compared to the tunica media. These microenvironments in which persistent

**Table 1** Microenvironmental distribution of *Borrelia burgdorferi* in the heart after antibody-mediated disease resolution

| Inoculum/immune serum <sup>a</sup> | Microenvironment              | Mean spirochete burden score $\pm$ s.e.m. |
|------------------------------------|-------------------------------|---|
| B31/B31                            | Tunica adventitia             | 0.2 $\pm$ 0.1 <sup>b</sup>                |
|                                    | Tunica media                  | — <sup>c</sup>                            |
|                                    | Myocardial connective tissues | 0.1 $\pm$ 0.1 <sup>d</sup>                |
| B31/NMS                            | Tunica adventitia             | 1.4 $\pm$ 0.3 <sup>b,c,d</sup>            |
|                                    | Tunica media                  | 0.3 $\pm$ 0.1                             |
|                                    | Myocardial connective tissues | 1.8 $\pm$ 0.4 <sup>b,c,d</sup>            |

Abbreviation: NMS, normal mouse serum.

Spirochete distribution and relative burden in the tunica adventitia, tunica media and myocardial connective tissue in C3H-*scid* mice at day 28 post inoculation.

<sup>a</sup>Mice were experimentally inoculated with *B. burgdorferi* strain B31 and passively immunized with either B31-specific immune serum or serum from uninfected naive mice.

<sup>b,c,d</sup>statistically significant differences (all *P*-values  $\leq$  0.05) between respective B31 serum-immunized and NMS treatment groups in specific microenvironments are identified by matching alphabets.

spirochetes localized are likely very similar, but only the tunica adventitia has been characterized. Based on comparative studies in human and laboratory rodents, the tunica adventitia of the aorta is composed of type I collagen, type III collagen, biglycan, decorin, and minimal type IV collagen.<sup>39–41</sup> The tunica media of the aorta contains all of the same ECM components except for the proteoglycan decorin.<sup>39,40,42</sup> There is indirect evidence to support a role for both decorin and type I collagen in determining the tissue specificity of persistent spirochetes. For example, an association between *B. burgdorferi* tissue burdens and decorin expression levels in homogenates of various tissues has been reported previously.<sup>27</sup> Additionally, type I collagen is commonly associated with decorin,<sup>18,39,40,43,44</sup> can independently form a matrix that permits borreliacolonization *in vitro*,<sup>25</sup> and corresponds with the distribution of decorin in certain rodent arteries.<sup>41</sup>

To evaluate the contributions of decorin and type I collagen in defining microenvironment-specific localization of spirochetes during chronic infection, the distribution of decorin and type I collagen was immunolocalized in naive C3H mice. Decorin immunolocalized to the tunica adventitia of the aorta (Figure 2a), and to the epicardium, endocardium, and myocardial interstitium (Figure 2b), corresponding with previously described decorin immunolocalization studies.<sup>39,40,42</sup> The distribution of collagen was next assessed by histochemistry and IHC. Using Masson's trichrome stain, collagen-rich connective tissue was identified in the tunica media and tunica adventitia of the aorta (Figure 3a) as well as the myocardial connective tissue (data not shown). The distribution of type I collagen, assessed by IHC, directly corresponded with the non-specific collagen staining with Masson's trichrome (Figure 3b). The pattern of decorin distribution (tunica adventitia and myocardial

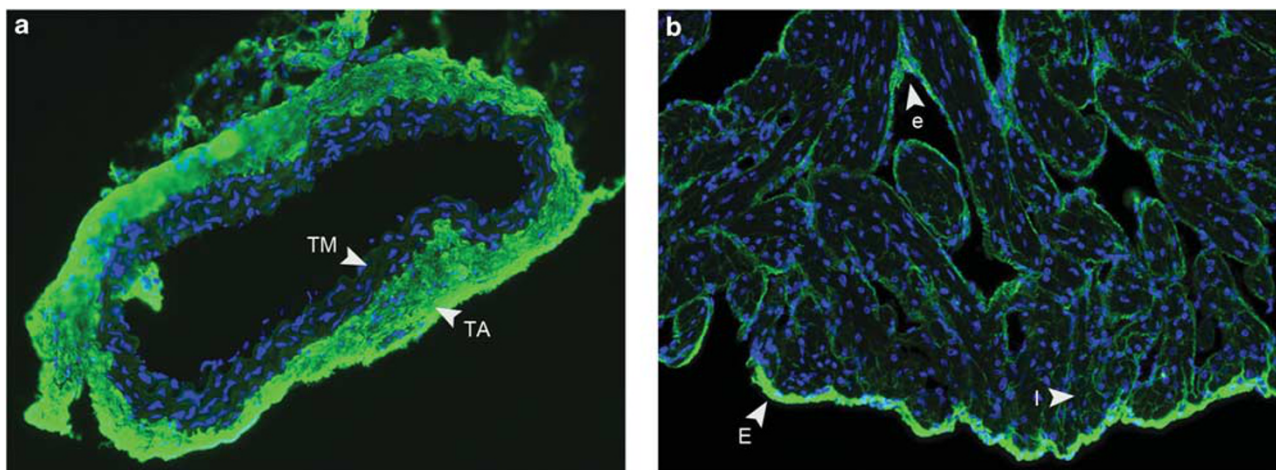


**Figure 2** Immunolocalization of decorin within cardiovascular connective tissues. Decorin was localized to (a) the tunica adventitia (TA) of the heart base aorta, and (b) the epicardium (E), endocardium (e) and myocardial interstitium (I) of the heart. Complete absence of immunofluorescence (IF) for decorin in the tunica media (TM) of the heart base aorta highlighted the close apposition of these decorin-rich and decorin-poor microenvironments. IF with goat anti-decorin primary antibody and NL493 fluorochrome-labelled secondary donkey anti-goat antibody; DAPI counterstain;  $\times$  20.

connective tissue only) was unchanged between naive mice and chronically infected C3H mice from the earlier study (Figure 3c). Microenvironmental colocalization of spirochetes and decorin (Figure 4) in the chronic stage of infection was demonstrated, further implicating decorin as a determining factor for defining permissive microenvironments. Based on these observations, *B. burgdorferi* preferentially localizes to connective tissue during early and chronic phases of infection, and decorin, not type I collagen, defines the connective-tissue microenvironment for persistence.

### Connective-Tissue Localization in Chronic Lyme Borreliosis is Dynamic

Within a discourse on the pathogenesis of chronic bacterial infections, Godfrey<sup>45</sup> proposed that localization of

microorganisms is dynamic, with bouts of acute infection arising from persistent and protected reservoirs to repopulate previously cleared and less-protected microenvironments. Microenvironmental localization in decorin-rich connective tissues could be an end-stage event, driven by humoral immunity and maintained as a static process. Alternatively, microenvironmental localization could be a dynamic event, as proposed by Godfrey.<sup>45</sup> To evaluate the dynamics of microenvironmental localization of *B. burgdorferi* in response to humoral immunity, the duration of infection in C3H-*scid* mice passively immunized with immune serum was extended to coincide with the time-dependent attrition of passively transferred immunoglobulins and thus, fading of humoral immunity. Thirty C3H-*scid* were inoculated with *B. burgdorferi* cN40 and 15 of these 30 C3H-*scid* mice were

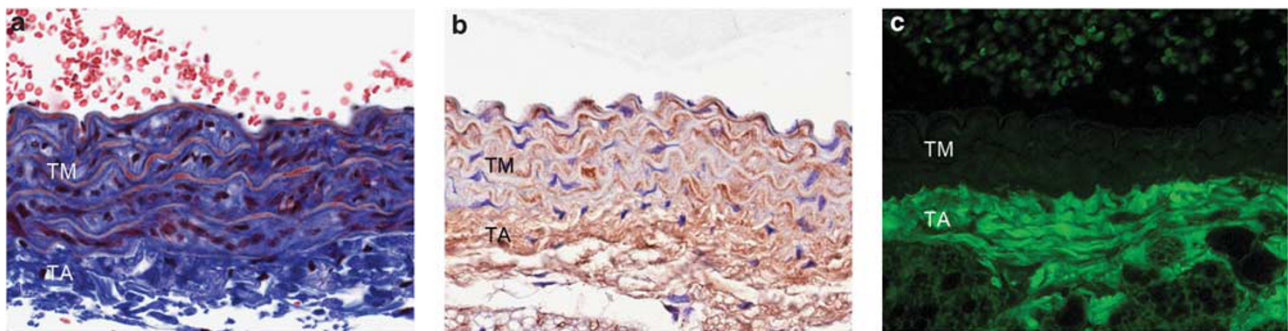


**Figure 3** Distribution of connective tissue (a), type I collagen (b), and decorin (c) in the heart base aorta of a C3H mouse, chronically infected (60 days post inoculation) with *B. burgdorferi*. Collagen-rich connective tissues and type I collagen were broadly distributed throughout the tunica adventitia (TA) and tunica media (TM). Decorin was restricted to the TA. Masson's trichrome (a), indirect IHC with polyclonal rabbit anti-type I collagen antibody and immunoperoxidase reaction with 3, 3'-diaminobenzidine (DAB) substrate (b), and IF with goat anti-decorin primary antibody and NL493 fluorochrome-labelled secondary donkey anti-goat antibody (c);  $\times 20$ .

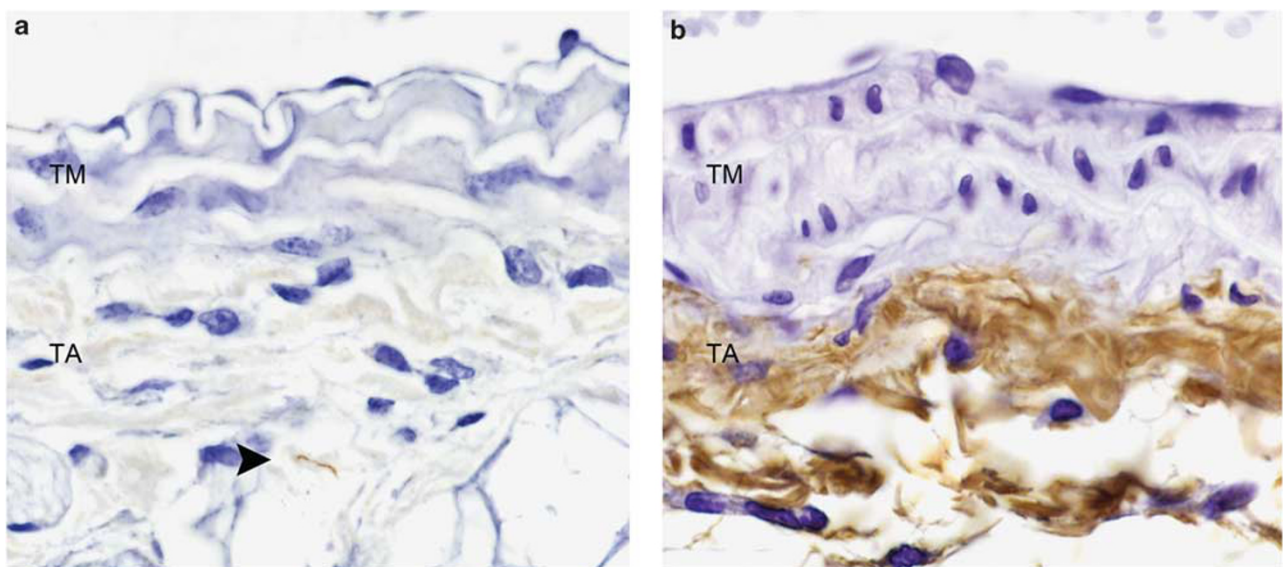


**Figure 4** Colocalization of persistent *B. burgdorferi* and decorin during chronic infection of an immunocompetent C3H mouse, at day 60 post inoculation. A single spirochete was identified in the tunica adventitia (a) of the heart base aorta (arrowhead). Restriction of decorin distribution to the tunica adventitia (b) remained constant over the duration of borreliosis. Indirect IHC with rabbit anti-*B. burgdorferi* immune serum or goat anti-decorin antibody and immunoperoxidase reaction with 3, 3'-diaminobenzidine (DAB) substrate; hematoxylin counterstain;  $\times 100$ .

passively immunized with either cN40-specific immune serum or NMS from uninfected mice. Subsets of five mice from each group were necropsied on days 28, 56, and 72 post inoculation (4, 32, and 48 days post serum administration). Day 72 was arbitrarily identified as the maximum duration of the experiment, based on progressively severe arthritis in C3H-*scid* mice administered NMS.

Total serum IgG levels (Figure 5a) progressively declined over time in the mice administered NMS (negative control group) and the mice passively immunized with N40-specific immune serum. Total serum IgG levels were consistently lower to undetectable in the negative control group. *B. burgdorferi* N40-specific antibody levels (Figure 5b) at day 28 were statistically significantly greater ( $P \leq 0.05$ ) than at days 56 and 72 in passively immunized mice, confirming successful transfer of *B. burgdorferi*-specific antibodies. At days 56 and 72, *B. burgdorferi* N40-specific antibody levels were near the minimum detection level and not significantly different from mice administered NMS. Therefore, the day 28 interval represented the established immune response and the day 56 and day 72 intervals represented decline of the *B. burgdorferi*-specific humoral immune response.

Passively transferred immune serum reduced, but did not clear, tissue spirochete burdens (Figures 6a–e) in the C3H-*scid* mice. At the initial time point, tissue burdens of spirochetes, based on copy numbers of *flaB* DNA per mg of tissue, in the passively immunized C3H-*scid* mice were lower than in NMS-treated C3H-*scid* mice. Over time, and with the waning of the antibody titer, tissue spirochete burdens proceeded to rise. The tissue spirochete burdens at the later time points, compared to the initial time point (day 56 and 72 versus day 28), were only significantly different in skin where tissue spirochete burdens were statistically significantly greater (Figure 6e). In NMS-treated C3H-*scid* mice, tissue burdens of spirochetes were initially higher, continued to progressively increase over time, and in many tissues, were significantly greater than in the passively immunized C3H-*scid* mice (Figures 6a, b and d).

At day 28 in the C3H-*scid* mice passively immunized with immune serum, spirochetes were identified by IHC within the tunica adventitia only (Table 2). No spirochetes were identifiable within the tunica media or the myocardial connective tissues. At day 28, the mean spirochete burden scores in all microenvironments were statistically significantly lower (all  $P$ -values  $\leq 0.05$ ) in mice treated with immune serum than in at least two of three microenvironments at all time points in the NMS-treated mice. In C3H-*scid* mice treated with immune serum, spirochetes were identified on days 56 and 72 within the previously cleared tunica media and the myocardial connective tissues. Identification of spirochetes in the tunica media on days 56 and 72 in C3H-*scid* mice treated with immune serum (Table 2) coincided with the decline of *B. burgdorferi*-specific antibody levels (Figure 5b). Though not significantly different from day 28, identification of spirochetes in the tunica media at days 56 and 72 was interpreted as repopulation of a previously cleared microenvironment. All microenvironments, especially the tunica media (Figure 7), at all time points were heavily populated by spirochetes in mice administered NMS, suggesting that one permissive condition for tissue colonization is the absence of borrelia-specific antibody. Thus, the data (repopulation of previously cleared microenvironments, rising spirochete tissue burden by *flaB* DNA copy number, and coincident decline in borrelia-specific antibody titer) suggest that recrudescence and re-invasion of previously cleared microenvironments occurs with waning humoral immunity.

## DISCUSSION

Using the heart as a tissue for investigation in the mouse model of chronic Lyme borreliosis, this study demonstrated a *B. burgdorferi*-specific antibody-driven change in microenvironmental localization of persisting spirochetes. Moreover, the antibody-driven change in borrelial microenvironmental sequestration was shown to be dynamic. With a decline of humoral immune pressure, recrudescence of persistent spirochetes resulted in the repopulation of

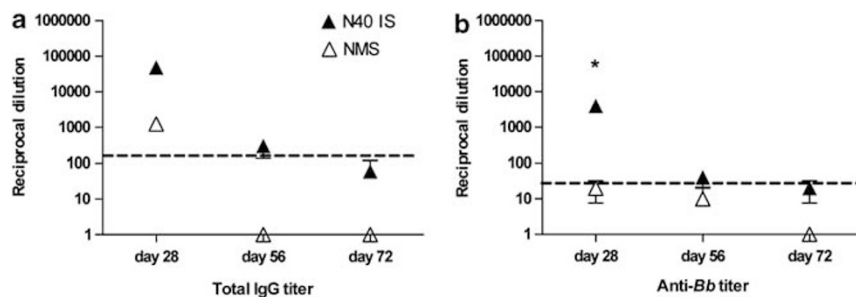


**Figure 5** Total IgG (a) and *B. burgdorferi*-specific (b) antibody titers waned over time in C3H-*scid* mice passively immunized with *B. burgdorferi* strain cN40-specific immune serum (N40 IS). Mice were inoculated with *B. burgdorferi* strain cN40 and immune serum was last administered on day 24 post inoculation. *Borrelia*-specific serum titers were significantly greater ( $*P \leq 0.05$ ) at day 28 but not significantly different from the negative control group (administered serum from naive uninfected mice, normal mouse serum (NMS)) at and after day 56 post inoculation. Each data point represents mean reciprocal dilution factor  $\pm$  s.e.m. from 4–5 mice.

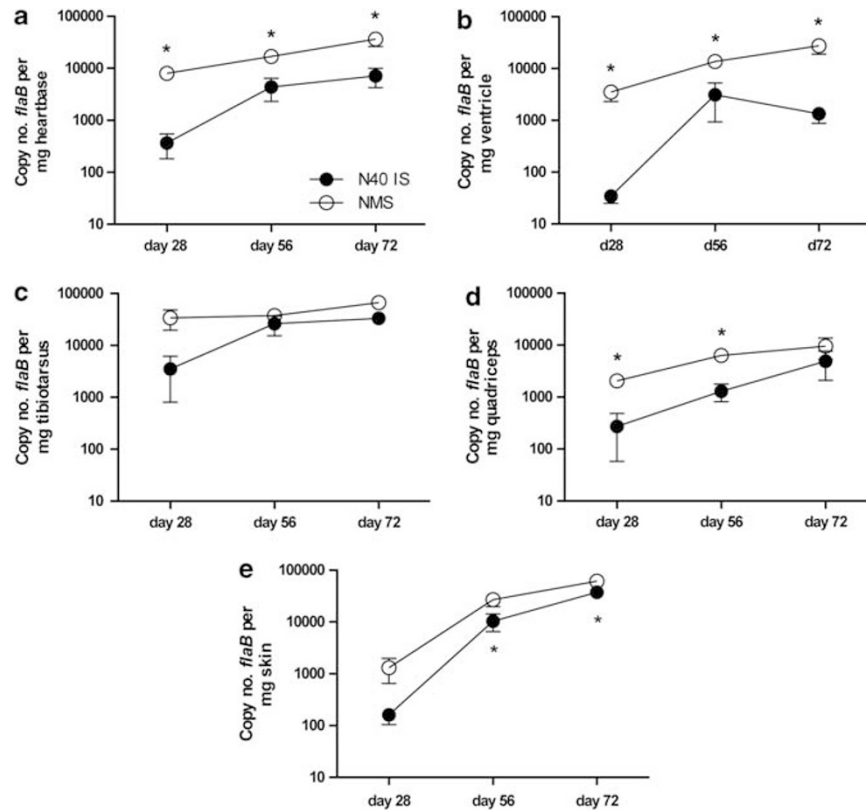


**Figure 6** Recrudescence of *B. burgdorferi* as the *B. burgdorferi*-specific antibody titer waned at and after day 56 post inoculation in passively immunized C3H-*scid* mice. The C3H-*scid* mice were inoculated with *B. burgdorferi* strain cN40 (N40 IS) and were administered cN40-specific immune serum or serum from naive uninfected mice (NMS) in three doses, ending on day 24 post inoculation. Tissue spirochete burdens (as the mean copy number *flaB* DNA  $\pm$  s.e.m.) rose in the heart base (a), ventricle (b), tibiotalarsus (c), quadriceps (d) and skin (e) as the antibody titer waned in the N40 IS-treated group, but only in skin (e) was the rise of spirochete tissue burdens statistically significant (\*all *P* values  $\leq$  0.05). As expected, in NMS-treated mice (negative control group) tissue spirochete burdens were statistically significantly greater in the heart base (a) (\*day 28, *P* < 0.013; day 56, *P* < 0.004; day 72, *P* < 0.024), ventricle (b) (\*day 28, *P* < 0.04; day 56, *P* < 0.007; day 72, *P* < 0.014) and quadriceps (d) (\*day 28, *P* < 0.004; day 56, *P* < 0.002).

antibody-cleared microenvironments. Finally, in this study, the recognized preferential connective-tissue localization of *B. burgdorferi* was confirmed and additional data were shown to support decorin as a significant determining factor of microenvironmental specificity.

The mechanism by which decorin defines protective microenvironments and prevents antibody clearance could be specific (due to antigen masking by binding to an immunogenic borrelial adhesin) or non-specific (by inhibiting antibody accessibility). Current evidence, including observations made in this study, supports the former possibility. A direct correlation between decorin expression in the homogenates of tissues and spirochete persistence has been observed in mice experimentally inoculated with *B. burgdorferi*,<sup>27</sup> but that study did not localize the specificity of the microenvironment. Greater tissue decorin expression levels were reported in sites (joint and skin) that harbored greater spirochete burdens during chronic infection ( $\sim$ 60 days) or after passive immunization with *B. burgdorferi*-specific immune serum. Decorin appeared to be the specific key component to these sites of sequestration, as these same

sites harbored significantly fewer spirochetes (by copy numbers of *flaB* DNA) in chronically infected decorin-deficient mice. Localization in these tissues could be driven by passive immunization of C3H-*scid* mice with polyclonal antibody to recombinant DbpA alone,<sup>6</sup> and these sites failed to protect spirochetes that expressed non-decorin-binding immunogenic adhesins (OspA and OspC),<sup>27,46</sup> indicating that the protective capacity of these tissues was not due to non-specific impermeability to antibody but was specific for Dbp-expressing spirochetes. Our findings further prove the importance of the decorin–spirochete colocalization, and extend this observation, showing that intact spirochetes were present within decorin-rich microenvironments and there is tissue redistribution with fluctuations in humoral immune pressure.

The role of Dbps and their specific interaction with the ECM and decorin in the pathogenesis of Lyme disease has been extensively investigated. The Dbps include a pair of outer surface proteins, DbpA and DbpB, that are constitutively expressed throughout all stages of infection,<sup>33,34,38,47</sup> are surface-exposed,<sup>19,38</sup> and are highly immunogenic.<sup>38,47,48</sup>



**Table 2** Loss of specific decorin-dependent connective-tissue localization during recrudescence of *Borrelia burgdorferi*

| Inoculum/immune serum <sup>a</sup> | Microenvironment              | Mean spirochete burden score $\pm$ s.e.m. |                            |                |
|------------------------------------|-------------------------------|---|----------------------------|----------------|
|                                    |                               | Day 28                                    | Day 56                     | Day 72         |
| N40/N40                            | Tunica adventitia             | 0.5 $\pm$ 0.3                             | 1.0                        | 1.0            |
|                                    | Tunica media                  | — <sup>b</sup>                            | 1.2 $\pm$ 0.5              | 0.8 $\pm$ 0.4  |
|                                    | Myocardial connective tissues | —   | 1.0                        | 0.9 $\pm$ 0.2  |
| N40/NMS                            | Tunica adventitia             | 1.8 $\pm$ 0.2                             | 1.0                        | 1.6 $\pm$ 0.3  |
|                                    | Tunica media                  | 1.0 $\pm$ 0.3                             | 2.8 $\pm$ 0.2 <sup>b</sup> | 3 <sup>b</sup> |
|                                    | Myocardial connective tissues | 1.4 $\pm$ 0.4                             | 1.6 $\pm$ 0.3              | 1.2 $\pm$ 0.2  |

Abbreviation: NMS, normal mouse serum.

As humoral immunity wanes, the previously cleared decorin-poor tunica media is repopulated.

<sup>a</sup>Spirochete distribution and relative burden in C3H-*scid* mice at days 28, 56 and 72 post inoculation, experimentally inoculated with *Borrelia burgdorferi* strain cN40 and passively immunized with cN40-specific immune serum or serum from uninfected naive mice.

<sup>b</sup>Statistically significant differences (all *P*-values  $\leq$  0.05) between N40 serum-immunized and NMS treatment groups within the respective micro-environments and durations of infection identified by matching alphabet.

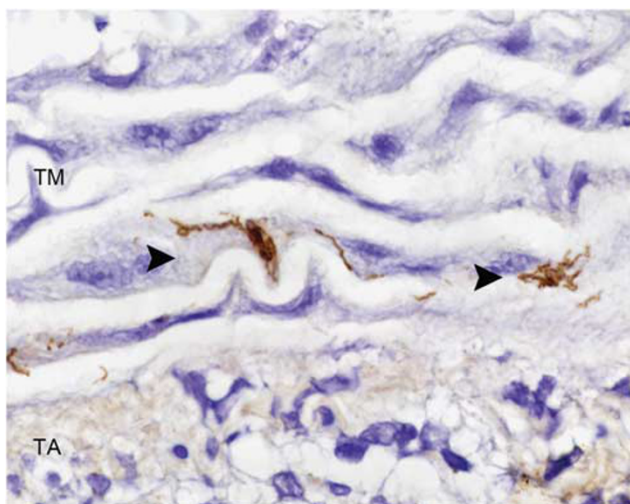


**Figure 7** Colonization of the decorin-poor tunica media (TM) by *B. burgdorferi* in a C3H-*scid* mouse administered with normal mouse serum (NMS), at day 72 post inoculation. Both single spirochetes and microcolonies (arrowheads) were present. Spirochetes also populated the tunica adventitia (TA). Indirect IHC with rabbit anti-*B. burgdorferi* immune serum and immunoperoxidase reaction with 3, 3'-diaminobenzidine (DAB) substrate; hematoxylin counterstain;  $\times$  40.

DbpA is considered to be the more biologically relevant adhesin, as it has a stronger specificity for the host ligand decorin,<sup>19</sup> induces stronger protective immunity,<sup>34,38</sup> can

solely induce a disease-resolving immune response,<sup>6</sup> and can restore a wild-type phenotype to Dbp-deficient mutant *Borrelia*.<sup>49–51</sup> Deficiency in Dbps results in a phenotype of delayed dissemination with an overall decrease in Dbp-deficient spirochete tissue burdens<sup>51,52</sup> and decreased retrieval of Dbp-deficient spirochetes from tissues distant to the inoculation site<sup>18,19,25</sup> at early time points (< 30 days). However, in the later stages of infection (> 42 days), tissue spirochete levels equivalent to wild-type infection are eventually reached and persistence is achieved by the Dbp-deficient spirochetes.<sup>51</sup> Thus, Dbps are involved in dissemination, are not absolutely required for persistence, and the phenotype of Dbp-deficient mutant *Borrelia* suggests the existence of functionally redundant adhesins that are involved in but less efficient at dissemination.

The lack of an absolute Dbp requirement for persistence does not negate the potential importance of the Dbp–decorin interaction in immune evasion. Rather, genetically manipulated spirochetes that lack a highly immunogenic, continuously expressed outer surface protein would be expected to evade immune clearance and persist. This scenario would be more likely to occur if there existed functionally redundant adhesins that may be less effective, but are not as immunogenic. Overproduction of either DbpA or DbpB has shown the opposite immunogenic pattern, with generation of a faster and stronger specific humoral immune response<sup>50,53</sup> and increased binding of specific antibodies to spirochetes.<sup>50</sup> Despite this, DbpA- and DbpB-overexpressing spirochetes are still not cleared and persist in a manner equivalent to the rescued wild-type phenotype of DbpA/B-complemented spirochetes.<sup>50</sup> In a separate study, spirochetes were shown to persist in lesser numbers and, predominantly, in the skin.<sup>53</sup> The DbpA-overexpressing mutant spirochetes share a phenotype of delayed dissemination with Dbp-deficient mutant spirochetes.<sup>50,53</sup> As one could postulate that the Dbp-deficient spirochetes are disseminating with the use of less-efficient functionally redundant adhesins, so, one could posit that the Dbp-overexpressing *Borrelia* may be slowed by increased interaction with the ECM. Increased interaction with the ECM (and decorin, specifically) may also explain why these extremely immunogenic, adhesin-overexpressing *Borrelia* may be able to avoid antibody-mediated clearance.

This study highlights the importance of the antigen-specific antibody response in Lyme borreliosis (reviewed by La Rocca *et al*<sup>54</sup>). The biphasic patterns of sequestration and subsequent recrudescence simultaneously occurring with the rise and fall of the *B. burgdorferi*-specific antibody titer suggest that the dynamics of persistence are at least partially dependent on humoral immune pressure. A similar phenomenon of recrudescence has been reported following passive transfer of neutralizing *B. burgdorferi* antigen-specific antibodies in immunodeficient mice.<sup>28</sup> The aforementioned study also demonstrated antibody-driven, antigen-dependent (OspC) positive selection of non-antigen expressing spirochetes with reversion to antigen expression after

antibody neutralization.<sup>28</sup> The antibody-driven immune pressure either induced downregulation or selected for a specific sub-population of *B. burgdorferi* that was then able to persist. A very similar phenomenon occurs in other borrelial species, such as the relapsing fever *Borrelia* spp., with cyclical proliferation and antibody clearance of one dominant serotype, only to allow another serotype to then proliferate.<sup>54</sup>

In this study, the phenomenon of recrudescence presented in the passively immunized C3H-*scid* mouse model is likely to be an exaggeration of what may occur in spontaneous infections. The biological validity of local recrudescence is supported by both clinical and experimental evidence of a cyclical disease pattern and a hyperimmunization antibody profile (suggestive of repetitive exposure) to chronic human and murine Lyme borreliosis.<sup>1,7,8</sup> The natural antibody profile reveals the caveats to local recrudescence in spontaneous Lyme disease. Bouts of untreated human Lyme arthritis typically occur in the face of a high antibody titer<sup>7,8</sup> suggesting that fluctuation in the quality of the antibody response, rather than quantity, is the determining factor for spirochetal repopulation of previously cleared microenvironments. Other cofactors, such as micro-trauma, within chronically infected joints may influence the episodic nature of clinical disease. Thus, we simply conclude that fluctuations in antibody-mediated immune pressure and recurrent bouts of local recrudescence arising from an internal reservoir of persistent bacteria may be one necessary factor in the maintenance of chronic borreliosis.<sup>45,55</sup>

#### ACKNOWLEDGEMENTS

We thank Kimberley Olsen, Edlin Escobar and Diane Naydan for their technical expertise and advice. This study was supported in part by NIH grants T32 AI 06055 (DI), T32 OD 011147 (DI), and R01 AI 26815 (SWB, SF, EH, KO).

#### DISCLOSURE/CONFLICT OF INTEREST

The authors declare no conflict of interest.

- Steere AC, Coburn J, Glickstein L. The emergence of Lyme disease. *J Clin Invest* 2004;113:1093–1101.
- Cabello FC, Godfrey HP, Newman SA. Hidden in plain sight: *Borrelia burgdorferi* and the extracellular matrix. *Trends Microbiol* 2007;15:350–354.
- Duray PH, Steere AC. Clinical pathologic correlations of Lyme disease by stage. *Ann NY Acad Sci* 1988;539:65–79.
- Barthold SW, Persing DH, Armstrong AL, et al. Kinetics of *Borrelia burgdorferi* dissemination and evolution of disease after intradermal inoculation of mice. *Am J Pathol* 1991;139:263–273.
- Shih CM, Pollack RJ, Telford SR, et al. Delayed dissemination of Lyme disease spirochetes from the site of deposition in the skin of mice. *J Infect Dis* 1992;166:827–831.
- Barthold SW, Hodzic E, Tunev S, et al. Antibody-mediated disease remission in the mouse model of Lyme borreliosis. *Infect Immun* 2006;74:4817–4825.
- Barthold SW, de Souza MS, Janotka JL, et al. Chronic Lyme borreliosis in the laboratory mouse. *Am J Pathol* 1993;143:959–971.
- Schoen RT. A case revealing the natural history of untreated Lyme disease. *Nat Rev Rheumatol* 2011;7:179–184.
- Nocton JJ, Dressler F, Rutledge BJ, et al. Detection of *Borrelia burgdorferi* DNA by polymerase chain reaction in synovial fluid from patients with Lyme arthritis. *N Engl J Med* 1994;330:229–234.
- Li X, McHugh GA, Damle N, et al. Burden and viability of *Borrelia burgdorferi* in skin and joints of patients with erythema migrans or Lyme arthritis. *Arthritis Rheum* 2011;63:2238–2247.
- Armstrong AL, Barthold SW, Persing DH, et al. Carditis in Lyme disease susceptible and resistant strains of laboratory mice infected with *Borrelia burgdorferi*. *Am J Trop Med Hyg* 1992;47:249–258.
- Cadavid D, O'Neill T, Schaefer H, et al. Localization of *Borrelia burgdorferi* in the nervous system and other organs in the nonhuman primate model of Lyme disease. *Lab Invest* 2000;80:1043–1054.
- Cadavid D, Bai Y, Hodzic E, et al. Cardiac involvement in non-human primates infected with the Lyme disease spirochete *Borrelia burgdorferi*. *Lab Invest* 2004;84:1439–1450.
- Imai DM, Barr BC, Daft B, et al. Lyme neuroborreliosis in 2 horses. *Vet Pathol* 2011;48:1151–1157.
- Alberts B, Johnson A, Lewis J, et al. *Molecular Biology of the Cell*. 4th edn, New York, NY, USA, 2002.
- Finlay BB, Falkow S. Common themes in microbial pathogenicity revisited. *Microbiol Mol Biol Rev* 1997;61:136–169.
- Antonara S, Ristow L, Coburn J. Adhesion mechanisms of *Borrelia burgdorferi*. *Adv Exp Med Biol* 2011;715:35–49.
- Guo BP, Norris SJ, Rosenberg LC, et al. Adherence of *Borrelia burgdorferi* to the proteoglycan decorin. *Infect Immun* 1995;63:3467–3472, 33.
- Guo BP, Brown EL, Dorward DW, et al. Decorin-binding adhesins from *Borrelia burgdorferi*. *Mol Microbiol* 1998;30:711–723, 38.
- Parveen N, Leong JM. Identification of a candidate glycosaminoglycan-binding adhesin of the Lyme disease spirochete *Borrelia burgdorferi*. *Mol Microbiol* 2000;35:1220–1234.
- Brissette CA, Bykowski T, Cooley AE, et al. *Borrelia burgdorferi* RevA antigen binds host fibronectin. *Infect Immun* 2009a;77:2802–2812.
- Verma A, Brissette CA, Bowman A, et al. *Borrelia burgdorferi* BmpA is a laminin-binding protein. *Infect Immun* 2009;77:4940–4946.
- Brissette CA, Verma A, Bowman A, et al. The *Borrelia burgdorferi* outer-surface protein ErpX binds mammalian laminin. *Microbiology* 2009b;155:863–872.
- Coburn J, Chege W, Magoun L, et al. Characterization of a candidate *Borrelia burgdorferi* b3-chain integrin ligand identified using phage display library. *Mol Microbiol* 1999;34:9266–9940.
- Zambrano MC, Beklemisheva AA, Bryksin AV, et al. *Borrelia burgdorferi* binds to, invades, and colonizes native type I collagen lattices. *Infect Immun* 2004;72:3138–3146, 34.
- Antonara S, Chafel RM, LaFrance M, et al. *Borrelia burgdorferi* adhesins identified using in vivo phage display. *Mol Microbiol* 2007;66:262–276.
- Liang FT, Brown EL, Wang T, et al. Protective niche for *Borrelia burgdorferi* to evade humoral immunity. *Am J Pathol* 2004;165:977–985.
- Liang FT, Jacobs MB, Bowers LC, et al. An immune evasion mechanism for spirochetal persistence in Lyme borreliosis. *J Exp Med* 2002;195:415–422.
- Barthold SW, Feng S, Bockenstedt LK, et al. Protective and arthritis-resolving activity in sera of mice infected with *Borrelia burgdorferi*. *Clin Infect Dis* 1997;25:S9–S17.
- Casjens S, Palmer N, van Vugt R, et al. A bacterial genome in flux: the twelve linear and nine circular extrachromosomal DNAs in an infectious isolate of the Lyme disease spirochete *Borrelia burgdorferi*. *Mol Microbiol* 2000;35:490–516.
- Fraser CM, Casjens S, Huang WM, et al. Genomic sequence of a Lyme disease spirochaete, *Borrelia burgdorferi*. *Nature* 1997;390:580–586.
- Barbour AG. Isolation and cultivation of Lyme disease spirochetes. *Yale J Biol Med* 1984;57:521–525.
- Hodzic E, Feng S, Freet KJ, et al. *Borrelia burgdorferi* population dynamics and prototype gene expression during infection of immunocompetent and immunodeficient mice. *Infect Immun* 2003;71:5042–5055.
- Feng S, Hodzic E, Stevenson B, et al. Humoral immunity to *Borrelia burgdorferi* N40 decorin binding proteins during infection in laboratory mice. *Infect Immun* 1998;66:2827–2835.
- Barthold SW, deSouza M, Feng S. Serum-mediated resolution of Lyme arthritis in mice. *Lab Invest* 1996;74:57–67.

36. Roberts WC, Mullikin BA, Lathigra R, *et al*. Molecular analysis of sequence heterogeneity among genes encoding decorin binding proteins A and B of *Borrelia burgdorferi* sensu lato. *Infect Immun* 1998;66:5275–5285.
37. Benoit VM, Fischer JR, Lin YP, *et al*. Allelic variation of the Lyme disease spirochete adhesin DbpA influences spirochetal binding to decorin, dermatan sulfate, and mammalian cells. *Infect Immun* 2011;79:3501–3509.
38. Hanson MS, Cassatt DR, Guo BP, *et al*. Active and passive immunity against *Borrelia burgdorferi* decorin binding protein A (DbpA) protects against infection. *Infect Immun* 1998;66:2143–2153.
39. Danielson KG, Baribault H, Holmes DF, *et al*. Targeted disruption of decorin leads to abnormal collagen fibril morphology and skin fragility. *J Cell Biol* 1997;136:729–743.
40. Reissen R, Isner JM, Blessing E, *et al*. Regional differences in the distribution of the proteoglycans biglycan and decorin in the extracellular matrix of atherosclerotic and restenotic human coronary arteries. *Am J Pathol* 1994;144:962–974.
41. Farquharson C, Robins SC. Immunolocalization of collagen types I and III in the arterial wall of the heart. *Histochem J* 1989;21:172–178.
42. Adhikari N, Carlson M, Lerman B, *et al*. Changes in expression of proteoglycan core proteins and heparin sulfate enzymes in the developing and adult murine aorta. *J Cardiovasc Trans Res* 2011;4:313–320.
43. Seidler DG, Dreier R. Decorin and its galactosaminoglycan chain: Extracellular regulator of cellular function? *IUBMB Life* 2008;60:729–733.
44. Bianco P, Fisher LW, Young MF, *et al*. Expression and localization of the two small proteoglycans biglycan and decorin in developing human skeletal and non-skeletal tissues. *J Histochem Cytochem* 1990;38:1549–1563.
45. Godfrey HP. Pathogenesis of chronic bacterial infections. *Trends Microbiol* 1998;6:303.
46. Strother KO, Hodzic E, Barthold SW, *et al*. Infection of mice with Lyme disease spirochetes constitutively producing outer surface proteins A and B. *Infect Immun* 2007;75:2786–2794.
47. Cassatt DR, Patel NK, Ulbrandt ND, *et al*. DbpA, but not OspA, is expressed by *Borrelia burgdorferi* during spirochetemia and is a target for protective antibodies. *Infect Immun* 1998;66:5379–5387.
48. Tunev SS, Hastey CJ, Hodzic E, *et al*. Lymphadenopathy during Lyme borreliosis is caused by spirochete migration-induced specific B cell activation. *PLoS Pathog* 2011;7:e1002066.
49. Shi Y, Xu Q, McShan K, *et al*. Both decorin-binding proteins A and B are critical for the overall virulence of *Borrelia burgdorferi*. *Infect Immun* 2008a;76:1239–1246.
50. Shi Y, Xu Q, Seemanapalli SV, *et al*. Common and unique contributions of decorin-binding proteins A and B to the overall virulence of *Borrelia burgdorferi*. *Plos One* 2008b;3:e3340.
51. Imai DM, Samuels DS, Feng S, *et al*. The early dissemination defect attributed to disruption of decorin-binding proteins is abolished in chronic murine Lyme borreliosis. *Infect Immun* 2013;81:1663–1673.
52. Weening EH, Parveen N, Trzeciakowski JP, *et al*. *Borrelia burgdorferi* lacking DbpBA exhibits an early survival defect during experimental infection. *Infect Immun* 2008;76:5694–5705.
53. Xu Q, Seemanapalli SV, McShan K, *et al*. Increasing the interaction of *Borrelia burgdorferi* with decorin significantly reduces the 50 percent infectious dose and severely impairs dissemination. *Infect Immun* 2007;75:4272–4281.
54. LaRocca TJ, Benach JL. The important and diverse roles of antibodies in the host response to *Borrelia* infections. *Curr Top Microbiol Immunol* 2008;319:63–103.
55. Young D, Hussell T, Dougan G. Chronic bacterial infections: living with unwanted guests. *Nat Immunol* 2002;3:1026–1032.